# Chain Segment Ordering in Swollen Polymer Brushes: Deuterium NMR Investigations

**Mehdi Zeghal,[†] Bertrand Deloche,*[,†] and Philippe Auroy*[,‡]**

*Laboratoire de Physique des Solides (CNRS-UMR 8502), Université Paris Sud, Orsay 91405, France, and Institut Curie, Section de Recherche (CNRS-UMR 168), 11 rue Pierre et Marie Curie, Paris 75005, France*

*Received July 21, 1998; Revised Manuscript Received February 22, 1999*

ABSTRACT: The dynamics of deuterated poly(dimethylsiloxane) chains grafted on a solid substrate and immersed in various solvents is investigated using deuterium NMR. It is observed that the segment reorientations are uniaxial around the normal to the grafting plane. For layers of moderate grafting density, immersed in poor solvent, the anisotropy is homogeneous and characterized by a negative order parameter *S*. The segment orientational fluctuations are preferentially parallel to the grafting plane through the whole layer. This anisotropy, due to the squeezing of the chains, depends on the average concentration of the polymer layer. On the contrary, in good solvent, the average order parameter is positive, indicating that the segments are preferentially oriented perpendicularly to the grafting plane. In this regime, the distribution of order $P(S)$ is broad and the chains are nonuniformly stretched.

## I. Introduction

Polymer brushes, formed by grafting polymers by one of their ends onto a surface, are of both fundamental and practical interest: the grafted chains may have configurations qualitatively very different from the case where they are in solution; grafted polymer layers can also be useful models to understand the behavior of polymeric surfactants, the stabilization of some colloidal suspensions, and the structures formed by block copolymers.

Following the seminal work of Alexander[1] and de Gennes,[2] a number of theoretical[3,4] and experimental studies of polymer brushes have been developed. A strong emphasis has been put on the structure of such grafted layers. For instance, it has been shown that the thickness $h$ of a polymer brush in good solvent scales as

$$h = aN\sigma^{1/3} \tag{1}$$

where $a$ is a monomer size, $N$ the number of monomers, and $\sigma$ the grafting density ($\sigma = a^2/D^2$, $D$ being the average distance between grafting sites). The development of small-angle neutron scattering (SANS)[5] and neutron reflectivity (NR)[6] techniques allowed the monomer density profile to be determined. But this type of information is still an average compared to the segmental level. More generally, little is known about the segment dynamics in thin polymer films, and in particular, the way the local dynamics is affected by the overall chain confinement is not well understood.

To probe molecular anisotropy, optical methods such as birefringence and dichroism are widely used.[7,8] Nevertheless, straightforward measurements of static birefringence or dichroism are unable to distinguish between uniform and nonuniform stretching.[7] On the contrary, deuterium NMR ($^2$H NMR), which has emerged as a powerful tool for probing local anisotropy in oriented polymers, is a well-suited experimental approach to characterize the distribution of order along nonuniformly constrained grafted chains.[9−11] In this work, we extended the same NMR approach developed previously for the study of end-grafted polymer layers in air: we investigated the segment dynamics of similar grafted layers immersed in various solvents.

We first describe the systems and the experimental methods (section II). The data obtained with a grafted monodomain of well-defined orientation with respect to the magnetic field and those obtained with a grafted porous silica are then presented and compared (section III). In particular, it is explained how the order distribution can be derived from the NMR spectra. This allowed us to compare the segmental dynamics of grafted polymer layers swollen by various solvents and to discuss the origin of the observed anisotropy (section IV).

## II. Experimental Section

**II.1. $^2$H NMR Background**. The basic concepts of deuterium NMR in anisotropic fluids have been developed in numerous references.[12,13] Only elementary results relevant for our purpose are recalled herein.

*Quadrupolar Interaction.* Due to its nonzero electric quadrupolar interaction, the deuterium ($^2$H) nucleus possesses an electrostatic energy in the nonuniform electric field of the C−D bond. This nuclear quadrupolar interaction is a second-order tensor affixed to the molecule; it is expressed by the instantaneous Hamiltonian:[14]

$$H_q = \frac{3}{2}\nu_q P_2(\Theta)(3I_z^2 - 2) \tag{2}$$

$I_z$ is the usual spin operator ($I^2 = 1$, so the effect of $H_q$ is to give a doublet of resonance lines). $\nu_q$, the static quadrupolar interaction constant, is 175 kHz. $\Theta$ is the instantaneous angle between the C−D bond and the steady magnetic field **B**, and $P_2(\Theta)$ denotes the second Legendre polynomial:

$$P_2(\Theta) = \frac{3\cos^2\Theta - 1}{2} \tag{3}$$

In the presence of molecular motions, a temporal average over

* To whom correspondence should be addressed.
[†] Université Paris Sud.
[‡] Institut Curie.

10.1021/ma981153y CCC: $18.00 
Published on Web 06/30/1999

fast segmental reorientations with respect to the inverse spectral width in the rigid lattice limit ($10^{-6}$–$10^{-5}$ s) must be considered in eq 2, leading to an average quadrupolar interaction $\Delta'$ given by

$$\Delta' = \frac{3}{2}\nu_q|\overline{P_2(\Theta)}| \tag{4}$$

Throughout the paper, overbars will denote temporal averages taken over rapid molecular motions. Note that $\Delta'$ is independent of **B** value.

*Relaxation Function*. Within this framework, and in the case of fast intrachain motions, the time evolution of the transverse magnetization (FID) for a deuterium nucleus may be written in the very simple form:

$$M(t) = M_0 e^{-t/T_2} \cos \Delta' t \tag{5}$$

If the motions of the C−D bond are isotropic (isotropic liquid), $\Delta'$ reduces to zero, and the transverse magnetic relaxation function is exponential with a relaxation time $T_2$. After Fourier transforming, the spectrum is a Lorentzian line of line width $(\pi T_2)^{-1}$. On the contrary, if the motions are anisotropic, the fluctuations no longer average the interaction $\Delta'$ to zero. This leads to a modulation of the transverse relaxation function, corresponding in the frequency domain to a doublet of Lorentzian lines symmetric relative to the Larmor frequency and characterized by a splitting $\Delta'$.

In the case of a nonuniform system, i.e., containing a C−D bond with distinct average axis and/or orientation degrees, there is one such doublet for each C−D bond (with a distinct orientation), and the resulting spectrum is the superposition of all these doublets. This *ensemble* average is denoted by angular brackets:

$$M(t) = M_0\langle e^{-t/T_2} \cos(\Delta' t)\rangle \tag{6}$$

Residual nuclear interactions $\Delta'$, even though they may be very weak compared to a true solid system, lead to a coherent or time reversible evolution which can be refocused by an appropriate pulse sequence. The resulting spectrum is inhomogeneously broadened by these interactions. The $T_2$ term is related to the fluctuating part of the Hamiltonian $H_q$ and leads to a homogeneous broadening of the NMR line. It corresponds to the irreversible contribution to the relaxation. Its measurement gives information on the dynamics of chain fluctuations. The $T_2$ contribution to the relaxation can be isolated using the quadrupolar echo sequence[15] which consists of two $\pi/2$ pulses ($\pi/2_x$, $\tau$, $\pi/2_y$, detect echo after $\tau$). This quadrupolar echo sequence is thus a good test to reveal anisotropic motions: in homogeneous magnetic field conditions, it gives rise to a pseudosolid echo when quadrupolar interaction is partially averaged by anisotropic motions. $T_2$ is the decay time of this pseudosolid echo.[16]

*Uniaxial Dynamics and Orientational Order*. The two steps described above must be clearly distinguished. First, the quadrupolar interaction for each nucleus is time averaged by fluctuations faster than $10^{-6}$–$10^{-5}$ s, leading to eq 4. Then, the relaxation function (eq 5) is integrated over all the nuclei present in the system, which leads to eq 6. The second step vanishes in a uniform uniaxial fluid system, wherein the motions of all C−D bonds consist of fast reorientational fluctuations around the same symmetry axis; in other words, all microscopic axes coincide with a macroscopic one, denoted by the unit vector **n**. In that case, the resulting spectrum is a unique doublet whose splitting $\Delta'$ may be expressed in frequency units as

$$\Delta' = \frac{3}{2}\nu_q|P_2(\Omega)||\overline{P_2(\theta)}| \tag{7}$$

where $\Omega$ is the angle between the symmetry axis **n** and the magnetic field, **B**, and $\theta$ is the angle between the C−D bond and **n**. The $P_2(\Omega)$ dependence may then be used as a crucial test for the uniaxial character of the molecular motions. $\overline{P_2(\theta)}$ is the mean degree of orientational order. It is the so-called order parameter $S$ which characterizes the anisotropy of the chain segments reorientational motions ($-0.5 \le S \le 1$). Equation 6 may also be written in term of effective interaction $\Delta$:

$$\Delta' = 2|P_2(\Omega)|\Delta \quad \text{and} \quad \Delta = \frac{3\nu_q}{4}|S| \tag{8}$$

The sign of the order parameter $S$ cannot be determined directly through $^2$H NMR spectra analysis. For instance, in the case of uniaxial dynamics, it is impossible in most of cases ($|S| \le 0.5$) to distinguish between segmental motions with a preferential orientation in the direction of the symmetry axis ($S > 0$) or normal to the symmetry axis ($S < 0$). The determination of the sign of $S$ requires to consider additional physical arguments such as the evolution of $|S|$ with the parameters of the system.

To have a better insight into molecular dynamics, it is generally more convenient to consider the order parameter of the local molecular axis, rather than the C−D bond order parameter. When the angular motional average in eq 6 involves fast uniaxial intramolecular rotations around a molecular symmetry axis, one gets

$$\overline{P_2(\theta(t))} = P_2(\gamma)\overline{P_2(\alpha(t))} \tag{9}$$

where $\gamma$ ($\alpha$) is the angle between the molecular symmetry direction and the C−D bond (and the macroscopic symmetry direction, respectively). The degree of anisotropy of the molecular axis reorientational motions is described by the order parameter $\overline{P_2(\alpha(t))}$.

In the particular case of poly(dimethylsiloxane) (PDMS), the Si−C bond is a symmetry axis for the methyl group rotations that involve tetrahedral angles ($\gamma_1 = 70.5°$). Then the line connecting two nearest oxygen atoms along the polymer backbone (normal to the Si−C bond, $\gamma_2 = 90°$) is treated as though it were a symmetry axis for the reorientations of the $Si(CD_3)_2$ group. On this assumption, the order parameter $S_{(O-O)}$ of this particular segment is

$$\frac{S_{O-O}}{S_{C-D}} = 6 \tag{10}$$

$$|S_{O-O}| = \frac{8\Delta}{\nu_q} \tag{11}$$

It is noticeable that the signs of $S_{C-D}$ and $S_{O-O}$ are the same. In comparison with $S_{C-D}$, $S_{O-O}$ is enhanced by a factor 6. Obviously, the choice of O−O segment as a molecular symmetry axis is not the only possibility. Other more realistic axis such as the backbone bonds can also be considered. The numerical value of the ratio in eq 10 depends on the considered molecular axis and is not crucial for the data interpretation.

**Table 1. Characteristics of the Grafted Layers in Air**[a]

| sample | $M_w$ | $I_w$ | $R_g$ (Å) | $D$ (Å) | $h_0$ (Å) |
|---|---|---|---|---|---|
| $M_t$ | 101 000 | 1.05 | 182 | 35.0 | 140.0 |
| $P_t$ | 77 500 | 1.04 | 153 | 36.6 | 89.0 |

[a] $M_w$ is the molecular weight of the grafted polymer, $I_w$ the polydispersity index, $R_g$ the radius of gyration of the same free chains in melt, $h_0$ the thickness of the grafted layer in air, and $D$ the average distance between grafting sites.

**II.2. Sample Preparation**. The sample characteristics and their elaboration, already described in a previous paper,[10] are only briefly recalled. The polymers we used are perdeuterated poly(dimethylsiloxane) (PDMS), synthesized via anionic polymerization. Their characteristics, determined by GPC, are indicated in Table 1. The polymer chains, terminated by a reactive end group, are covalently bound to the silica surface. The substrates are either planar glass slides (sample $M_t$ in

Table 1) or porous silica (specific surface area 1.8 $m^2/cm^3$, pore size 400 nm, sample $P_t$ in Table 1). For both kinds of samples, the surface has been treated in order to reduce the polymer adsorption.

To increase the NMR signal-to-noise ratio, the glass slides (about 50) are stacked in a cylindrical rack as described in ref 9. This provides us with a monodomain of well-defined orientation with respect to the magnetic field of the NMR spectrometer. The porous silica, on the contrary, has a randomly oriented surface.

To determine the amount of grafted polymer, we used small-angle neutron scattering (SANS) for the porous silica and X-ray reflectivity for the glass slides. The dry layer thickness and the corresponding average distance $D$ between grafting sites are reported in Table 1.

**II.3. NMR Equipment and Data Acquisition Method.** This $^2H$ NMR study was done at room temperature, well above the crystallization temperature of PDMS (236 K). Experiments were performed either on a Bruker MSL-400 operating at 65 MHz or on a modified Bruker CXP 90 spectrometer operating at 13 MHz and using an electromagnet locked at 2 T. The magnetic field inhomogeneity was estimated to be less than 10 Hz at 13 MHz ($\Delta B/B < 10^{-6}$) over the volume of porous silica (0.5 $cm^3$). We checked that the line broadening induced by porous silica on a low molecular weight polymer melt spectrum is lower than 5 Hz.

Using the slides rack described in ref 9, the orientation of the monodomain sample relative to the magnetic field is fixed for experiments performed at 65 MHz ($\Omega = 90°$) and adjusted with a goniometer (angular accuracy of $\pm 1°$) for experiments performed at 13 MHz.

Both types of substrate (monodomain of glass slides and porous silica) are of complementary use: the monodomain allows us to fully characterize the segment dynamics. But only nonprotonated solvents (like $CCl_4$) can be used: regular organic solvents (like methanol or hexane) are excluded because of their natural deuterium content which would hide the signal of the grafted layer. On the other hand, the interpretation of the NMR spectra is less straightforward with the porous silica because the surface is randomly oriented with respect to the magnetic field, but given the high specific surface area of the sample, systematic experiments can be performed as well as relaxation measurements. For the latter experiments, because of the signal weakness, the echo amplitude decay hardly exceeds 1 decade. The $T_2$ measurements were performed in homogeneous magnetic field conditions, using the quadrupolar echo sequence quoted in section II.1. We checked that, for a low molecular weight PDMS melt ($\Delta = 0$), the relaxation functions obtained with this pulse sequence and with a simple Hahn echo sequence are monoexponential and exhibit the same $T_2$ relaxation time.

## III. Results

The results obtained with the monodomain are first described. Only two cases are considered: in air (which can be seen as the worst solvent) and in good solvent for the grafted chains. More systematic studies have been performed with the porous silica in poor and good solvents of PDMS:[17] they are presented in the second subsection. In the last section of this third part, the line shapes of the different spectra are quantitatively analyzed in terms of order distribution.

**III.1. Monodomain.** *In Air.* Figure 1a shows the spectrum obtained with the glass slides (monodomain $M_t$ in Table 1) in air for an angle $\Omega = 90°$ between the normal to the substrate and the magnetic field. The most striking feature is that a well-resolved doublet appears ($\Delta \neq 0$). It has already been pointed out in refs 9 and 10 that the doublet spacing reproduces with a great accuracy the $P_2(\Omega)$ dependence stressed in eq 7. This demonstrates that the motions of the chain segments are uniaxial around the normal to the flat

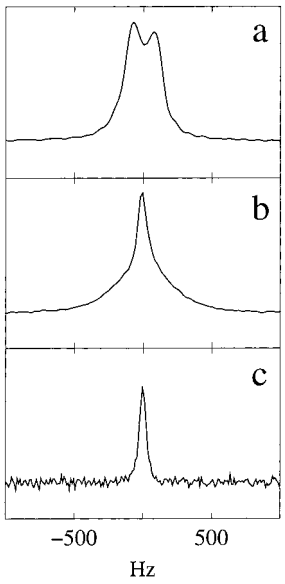


**Figure 1.** (a) The 65 MHz $^2H$ NMR spectrum of sample $M_t$ in air for $\Omega = 90°$. (b) The 65 MHz $^2H$ NMR spectrum of sample $M_t$ in $CCl_4$ for $\Omega = 90°$. (c) The 13 MHz $^2H$ NMR spectrum of sample $M_t$ in $CCl_4$ for $\Omega = 55°$.

substrate. Moreover, studies versus dry layer thickness demonstrate that this motional uniaxiality in grafted melts is characterized by a negative order parameter ($S_{(O-O)} < 0$) (see ref 10): the segment orientational fluctuations are preferentially parallel to the grafting plane throughout the whole layer. This effect is related to the squeezing of the chains between the sharp silica−polymer and polymer−air interfaces.

*In Good Solvent.* Figure 1b displays the $^2H$ NMR spectrum obtained with $M_t$ immersed in $CCl_4$, for $\Omega = 90°$. This spectrum is very different compared to the dry case, indicating that the segmental dynamics is radically modified by the swelling of the grafted layer. Instead of a doublet structure, we observe a single symmetric resonance line with broad wings. This "super Lorentzian" line shape differs strongly from the narrow liquid-like resonance line observed on free chains in melt or in solution.[10] Moreover, the half-height line width $\delta\nu$ is much higher than the homogeneous line broadening ($1/\pi T_2$) corresponding to the transverse relaxation time $T_2$ measured with the porous silica immersed in a good solvent (see section III.2). These observations suggest that the broadening of the spectrum in good solvent is also due to nuclear interactions which are not completely time averaged. This is confirmed by changing $\Omega$: the spectrum obtained for $\Omega = 55°$ is displayed in Figure 1c. The magic angle narrowing effect shows unambiguously that the normal to the flat substrate remains a symmetry axis for the segment motions. It also proves that the spectrum observed at $\Omega = 90°$ results from a broad distribution of doublets (whereas in air, the distribution is narrow enough to give rise to a unique well-resolved splitting). A more quantitative analysis of this distribution will be discussed below.

It has been shown theoretically[1−3] and experimentally[4−6] that, in a polymer brush immersed in a good solvent, the chains are strongly stretched. This might be the source of the anisotropy we observed for $M_t$ in $CCl_4$: in that case, the segment orientational fluctuations would be preferentially perpendicular to the grafting surface. This means that the order parameter $S_{(O-O)}$ (denoted $S$ in the following) would be positive in

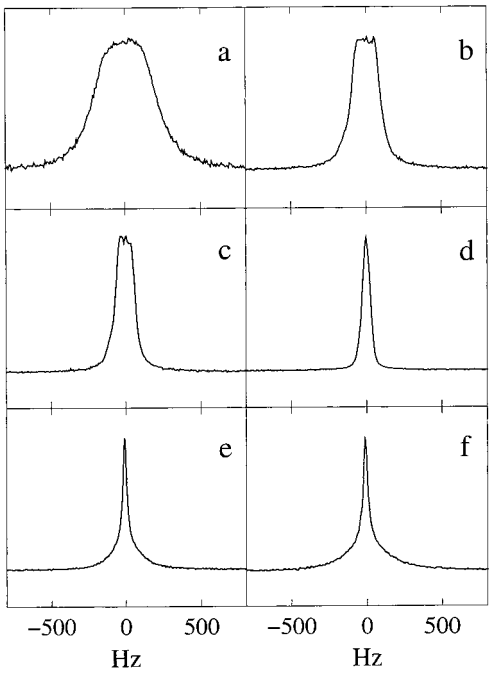


**Figure 2.** The 13 MHz $^2$H NMR spectrum of sample $P_t$ in various solvents: (a) in air; (b) in methanol; (c) in ethanol; (d) in acetone; (e) in toluene; (f) in hexane.

good solvent. Since we already saw that in air $S$ is negative due to the squeezing of the chains, we expect that if we use solvents of increasing quality from air (which can be considered as a very poor solvent) up to a very good solvent like hexane, $S$ should change its sign. As mentioned in section II.1, the sign of $S$ cannot be directly determined from spectrum analysis. However, such a sign change would induce a nonmonotonic solvent quality dependence of $|S|$. More precisely, the magnitude of the order parameter is expected to decrease first to zero and then to increase again. This observation cannot be easily done with the monodomain because the small amount of deuterium in the sample limits us to nonprotonated solvents. This however would be straightforward with the porous silica as will be shown in the following.

**III.2. Grafted Porous Silica.** *In Air.* Figure 2a shows the $^2$H NMR spectrum obtained with the porous silica (sample $P_t$; see Table 1) without solvent. The broad non-Lorentzian line shape ($\delta\nu = 400$ Hz) is again related to an incomplete time averaging of quadrupolar interactions due to uniaxial motions along the normal to the substrate.[10,11] It has been shown that this spectrum can be accurately reproduced by averaging over all the (random) orientations of the porous silica the doublet structure obtained with a monodomain of similar characteristics.[10]

*In Poor Solvent.* What happens to the $^2$H NMR spectrum if this grafted porous silica is immersed in different poor solvents of increasing quality? In Figure 2b−d are displayed the results obtained with methanol, ethanol, and acetone, which are all poor solvents of PDMS but of increasing quality. For the whole series, the line shape is rather unusual compared to what is obtained for polymer chains in solution. In all cases, the half-height line width $\delta\nu$ is much larger than the homogeneous broadening ($1/\pi T_2 < 20$ Hz). Indeed, we also performed $T_2$ measurements for this porous silica in the same three solvents: We observed a pseudosolid echo as a response to the quadrupolar echo sequence

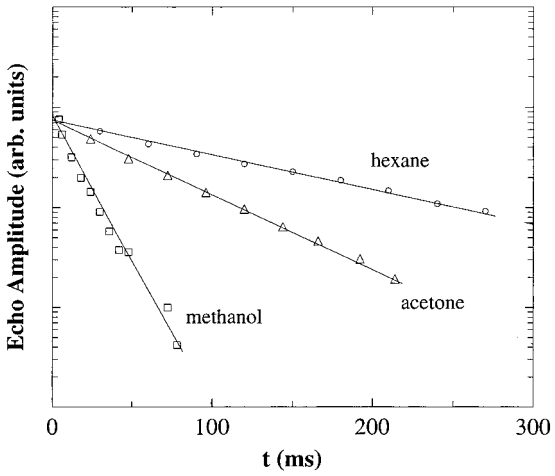


**Figure 3.** Semilog plots of the echo amplitude (au) measured at the maximum, as a function of the time interval $\tau$ of the solid echo pulse sequence. These relaxation functions were obtained on sample $P_t$ in methanol, acetone, and hexane.

(data not shown), whose relaxation is characterized by a single time (Figure 3). Therefore, the broadening of the NMR spectra in poor solvent is also due to residual quadrupolar interactions related to anisotropic motions. This makes the comparison of the different spectra sound: the spectral width $\delta\nu$ appears to be a decreasing function of the solvent quality (including air which is the worst in this series of poor solvents).

*Polymer Brush in Good Solvent.* The spectra obtained with $P_t$ immersed in toluene and hexane, good solvents for PDMS (hexane is a better solvent than toluene[18]), are displayed in Figure 2, e and f, respectively. Their line shape differs radically from those observed in poor solvent and discussed above. Mainly, they present a wide base topped by a narrow line. As previously, the broadening is larger than the liquid line width $1/\pi T_2$ where $T_2$ is the characteristic decay time of the pseudosolid echo (see Figure 3). These results are consistent with the observations made on the monodomain in $CCl_4$: they demonstrate that the segment motions are anisotropic on the $^2$H NMR time scale (less than $10^{-6}$−$10^{-5}$ s). In addition, we can notice a clear widening of the spectrum base from acetone to toluene and from toluene to hexane. The spectrum obtained with $P_t$ in $CCl_4$ is not shown here since it is identical to the one obtained in hexane. This indicates that the average anisotropy increases with the solvent quality, contrary to the behavior observed in poor solvent. Besides, the appearance of a narrow component at the Larmor frequency suggests that somewhere along the grafted chains isotropic motions take place.

**III.3. NMR Line Shape and Distribution of Order.** To fully characterize the anisotropy revealed by the NMR spectra, it is worth extracting the order distribution from the NMR line shapes. This can be done on spectra obtained with the monodomain as well as with the grafted porous silica. In the latter case, the random distribution of the local normal to the substrate must be introduced.[10,11] In all cases, the $T_2$ term contribution used for these calculations was measured using the solid echo pulse sequence (see section II.1 and Figure 3). The type of distribution of residual quadrupolar interaction $P(\Delta)$ used to fit the experimental data is chosen arbitrarily, but in each case, the choice is justified a posteriori by the quality of the fits.

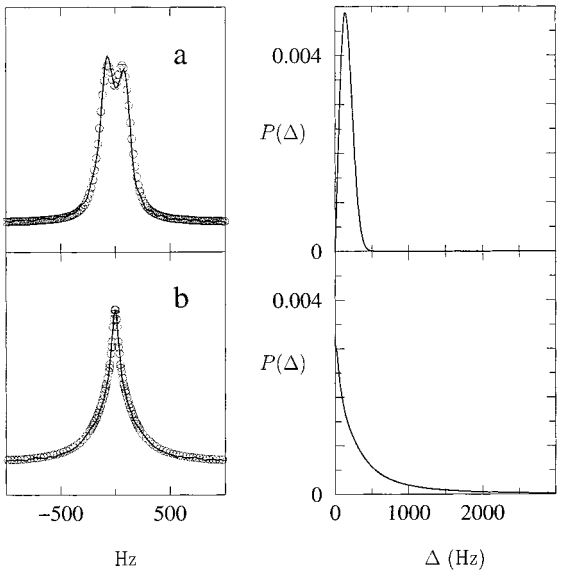


**Figure 4.** On the left are displayed the 65 MHz $^2$H NMR spectra (solid line) obtained with $M_t$ (a) in air and (b) in $CCl_4$, both for $\Omega = 90°$. They were fit (open circles) using the distributions of residual interactions $P(\Delta)$ shown on the right.

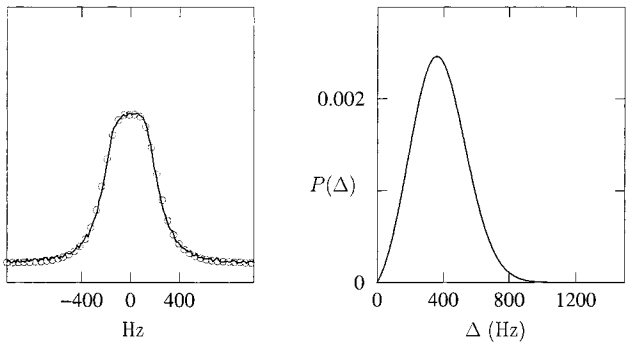


**Figure 5.** On the left is displayed the 13 MHz $^2$H NMR spectrum (solid line) obtained with $P_t$ in air. It was fit (open circles) using the distribution of residual interactions $P(\Delta)$ shown on the right. The expression of $P(\Delta)$ is given in eq 12. The output of the fit is $\Delta_0 = 260$ Hz, $\sigma = 190$ Hz.

*Poor Solvent Regime.* To fit the spectra obtained on the grafted layers in air, we used the following distribution, as in ref 10:

$$P(\Delta) \propto \Delta e^{-(\Delta-\Delta_0)^2/2\sigma_2}, \quad \text{with } \Delta > 0 \qquad (12)$$

where $\Delta_0$ and $\sigma$ are adjustable parameters. For both the monodomain and the porous silica, the fits are satisfactory (see Figure 4a back to Figure 1a, and Figure 5 back to Figure 2a).

This procedure was extended to reproduce the spectra obtained in poor solvent. Attempts at fitting the spectra by the same $P(\Delta)$ function proved unsuccessful. On the other hand, as shown in Figure 6, the agreement between the simulated and the experimental spectra becomes excellent by using the following distribution:

$$P(\Delta) \propto \frac{\Delta^{0.5}}{1 + \dfrac{(\Delta - \Delta_0)^2}{\sigma^2}}, \quad \text{with } \Delta > 0 \qquad (13)$$

It is noticeable in Figure 6 (back to Figure 2b−d) that the anisotropy distribution is much narrower when the layer is immersed in a solvent than in air. Furthermore,

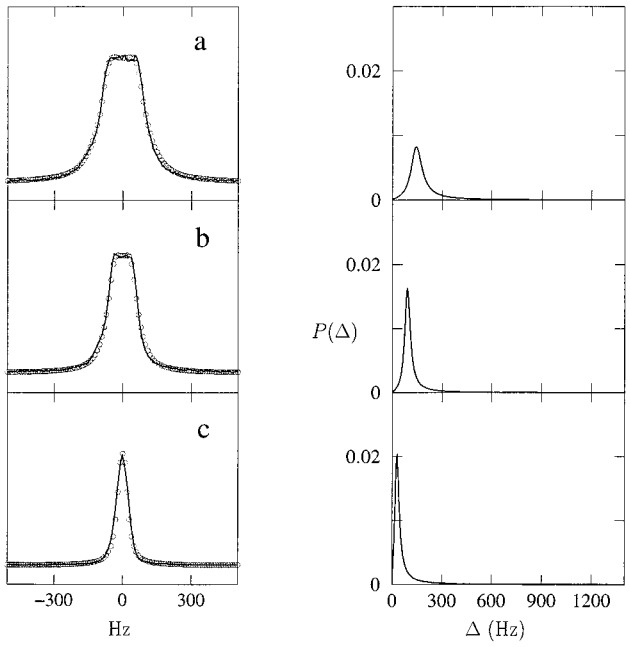


**Figure 6.** On the left are displayed the 13 MHz $^2$H NMR spectra (solid line) obtained with $P_t$ (a) in methanol, (b) in ethanol, and (c) in acetone. They were fit (open circles) using the distribution of residual interactions $P(\Delta)$ shown on the right (eq 13). The output of the fit is $\Delta_0 = 140$ Hz, $\sigma = 40$ Hz in methanol; $\Delta_0 = 90$ Hz, $\sigma = 20$ Hz in ethanol; and $\Delta_0 = 27$ Hz, $\sigma = 16$ Hz in acetone.

when the distribution width is smaller than the average $\Delta$ value, the particular "square" line shape of the top of the spectra is well reproduced. Another important feature is the absence of any isotropic component in $P(\Delta)$, even for acetone. This is confirmed experimentally by the presence of a pseudosolid echo at long delay times ($\tau > 7$ ms). Finally, the variation of the anisotropy with the solvent quality is directly observable on the plotted distributions: the average degree of order is a decreasing function of the solvent quality in poor solvent regime.

*Good Solvent Regime.* As already pointed out, the spectra in good solvent strongly differ from those of the previous regime. A Lorentzian distribution, centered at $\Delta = 0$

$$P(\Delta) \propto \frac{1}{1 + \dfrac{\Delta^2}{\sigma^2}}, \quad \text{with } 0 < \Delta < \Delta_{max} \qquad (14)$$

allows us to fit the NMR data. Indeed, the agreement between the spectrum simulated using this $P(\Delta)$ and the experimental results is good both for the monodomain (Figure 4b back to Figure 1b) and for the porous silica (Figure 7a,b back to Figure 2e,f). For greater convenience, we fixed $\Delta_{max} = 20$ kHz, which corresponds to $S = 1$ in eq 11. This upper value $\Delta_{max}$ is somewhat arbitrary, but it does affect neither the quality of the fits nor the normalization constant for $P(\Delta)$, provided it is high enough. Contrary to what has been observed in poor solvent, the anisotropy increases with the solvent quality as can be clearly seen on the distributions displayed in Figure 7a,b (back to Figure 2e,f). Moreover, the contribution of isotropic or slightly anisotropic segmental motions is significant in this regime.

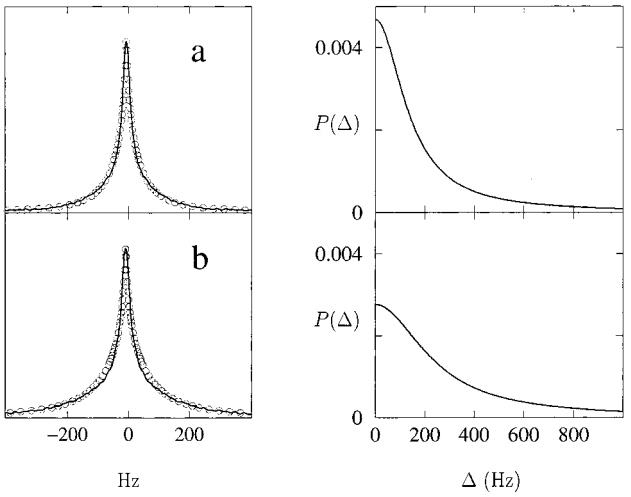


**Figure 7.** On the left are displayed the 13 MHz $^2$H NMR spectra (solid line) obtained with $P_t$ (a) in toluene and (b) in hexane. They were fit (open circles) using the Lorentzian distribution (eq 14) of residual interactions $P(\Delta)$, centered at $\Delta_0 = 0$, shown on the right (eq 14). The output of the fit is $\sigma =$ 140 Hz in toluene and $\sigma = 240$ Hz in hexane.

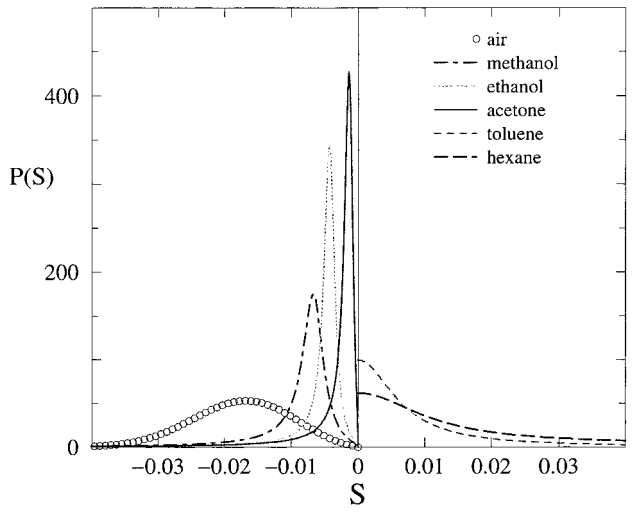


**Figure 8.** Distribution of order parameter $P(S)$ in various solvents. $S$ is the order parameter of the O−O segment along the PDMS chain. $P(S)$ was derived from $P(\Delta)$ and eq 11.

## IV. Discussion

In a preceding work, we showed that a grafted polymer layer in air exhibits uniaxial dynamics, the anisotropy being a decreasing function of the grafting density.[9,10] This was interpreted as a consequence of the squeezing of the polymer between two sharp interfaces. Indeed, for the samples we investigated, the thickness $h$ of the grafted layer in air was smaller than or comparable to the unperturbed radius of gyration $R_g$. We observed that the order parameter (characterizing the anisotropy of the segment dynamics) was correlated to the squeezing ratio $h/R_g$ (the smaller this ratio, the larger the order parameter). This uniaxial segment dynamics corresponds to reorientational fluctuations that are parallel to the surfaces; the order parameter $S_{(O-O)}$ is thus negative.

In this paper, we have extended this investigation to various solvents. For a given sample ($P_t$), we observed that the line width decreases following the sequence air, methanol, ethanol, and acetone which are poor solvents of increasing quality. This result is in perfect agreement with the interpretation of the anisotropy in terms of squeezing (that we had proposed for the results obtained with a series of grafted layers in air). Indeed, in this sequence of solvents, the thickness of the grafted layer increases (as we go from air to acetone): more and more solvent penetrates into the polymer interface. Thus, the squeezing ratio increases which indeed corresponds to the decrease of the observed degree of order.

We also noticed that the order parameter distribution $P(S)$ is narrow in all the poor solvents of the above-mentioned series (see Figure 8): this tells us that the squeezing constraint is quite uniformly distributed along the normal to the surface.

How can our results be compared with the theoretical predictions made on brushes in poor solvents?[4,19] Unfortunately, there is no real overlap. Indeed, all the theoretical studies considered the strong stretching regime where $h/R_g \gg 1$. But our samples do not satisfy this criterion in poor solvent; on the contrary, we showed that the squeezing of the chains is the main source of anisotropy.

In addition to the squeezing, there must be some other contributions that would affect the segment ordering. Indeed, by comparison with grafted layers in air, it is noticeable that for the same $h/R_g$ the degree of order measured in poor solvent is significantly smaller. Let us consider for instance the case of sample $P_t$ immersed in methanol for which the ratio $h/R_g$ increases by about 10%[20] but the order parameter $S$ is reduced by a factor 2 with respect to the dry layer. Similarly, the line width observed with the sample $P_t$ of this paper in acetone ($\delta\nu = 60$ Hz, $D = 36.6$ Å, $h/R_g = 0.88$) is smaller than the one already measured on a sample of higher grafting density in air[10] ($\delta\nu = 160$ Hz, $D = 28.2$ Å, same polymer, $h/R_g = 0.98$), which has a greater $h/R_g$. What could these additional contributions be?

Theoretical studies suggest that a strong orientation is induced for chain segments that are close to an impenetrable wall1,[21−23] the extreme limit being a perfect in plane alignement ($S = -0.5$). Hence, in dry layers, the chain segments located in the immediate vicinity of the silica−polymer and polymer−air sharp interfaces are expected to be fully oriented. In poor solvent, as revealed by SANS and NR studies, the polymer interface is less and less steep as the solvent quality increases: the polymer−solvent boundary is less and less well-defined, and similarly, a depletion layer of increasing width appears at the solid−polymer interface. Therefore, the segment orientation induced at these boundaries must be less and less strong.

The above-mentioned steric effect is supposed to be of short range,[21−23] typically a few persistence lengths (i.e., a few segments for PDMS). In our case, the NMR spectra and the inferred order distributions clearly indicate that the segmental order persists through the entire layer. This experimental fact, together with the observed dynamical uniaxiality, can be considered as evidence for orientational interactions between segments. It is important to mention that this phenomenon, already revealed in other confined polymer systems (as uniaxially strained networks), depends strongly on the local density of chain segments.[24,25] In other words, the orientation coupling between segments is partially screened upon dilution. This screening effect can contribute to reduce the local order.

Another striking result that deserves to be discussed is the clear tendency for poor solvents to make the order

distribution $P(S)$ narrow in comparison with the dry layer (see Figure 8); furthermore, such a narrowing effect increases with the solvent quality. As was pointed out in a previous work,[10] the order distribution is associated with a gradient along the normal to the substrate. The order near the sharp interfaces is maximum and decreases as we go into the inner of the layer. Adding a solvent to polymer chains generally increases the chain mobility as reflected by the dependence of $T_2$ with solvent quality (see Figure 3): the solvent molecules allow chain segments to diffuse over larger distances during the $^2$H NMR time scale ($10^{-6}$ s). Thus, the average is made over larger distances along the direction of the order gradient (the $z$ axis), inducing a narrowing effect on $P(S)$.

If we use solvents of increasing quality, we first observe a decrease (poor solvent regime) and then an increase (good solvent regime) of the anisotropy. This means that the average order parameter $\langle S \rangle$, which is negative in air (very poor solvent), must change its sign in good solvent (see Figure 8). In other words, the preferred orientation of the segment dynamics switches from parallel (in air) to perpendicular (in good solvent)—with respect to the silica surface. This perpendicular orientation can be explained by the strong stretching of the grafted chains in good solvent. This transition implies that, for a given value $\chi^*$ of the Flory interaction parameter ($\chi < 0.5$) corresponding to $\langle S \rangle = 0$, the constraints exerted on the grafted chains must be released: the polymer chains would adopt a nearly isotropic conformation. Experimentally, this would be associated with a perfect liquidlike NMR spectrum ($\Delta = 0$). For the sample $P_t$ studied here, this would occur with a solvent slightly better than acetone.

Although the order distributions are very different in poor and good solvent, the $T_2$ relaxation remains monoexponential (see Figure 3), with a characteristic decay time that is drastically reduced as the solvent quality is lowered. This $T_2$ variation indicates that the chain mobility is hindered as the rate of swelling decreases. This observation is consistent with the interpretation in terms of chain squeezing.

From the (broad) order distribution $P(S)$ measured in good solvent (see Figure 8), it is worth trying to extract the order profile $S(i)$ along the chain backbone, $i$ being the $i$th segment along the chain starting from the silica surface. Assuming that the segmental anisotropy is a decreasing function of the index $i$, this is in principle achievable. But the uncertainty on the value of $S$ at the grafting plane makes this determination not very accurate. Nevertheless, it remains possible to compare experimental NMR spectra with spectra calculated using theoretical order profiles. For polymer brushes in good solvent, within a self-consistent-field approach,[4,7] the average position $z(i)$ of the $i$th segment is given by

$$z(i) = z(N) \sin\left(\frac{i\pi}{2N}\right) \tag{15}$$

where $z(N)$ is the distribution of free ends within the layer.

The local order parameter $S(i)$ is given by

$$S(i) = \frac{3}{2a^2}\left(\frac{\partial z(i)}{\partial i}\right)^2 \tag{16}$$

where $a$ is the segment size and $\partial(z(i))/\partial i$ the local chain stretching at a distance $z$. Taking into account the distribution of free ends $z(N)$, one gets the order parameter profile along the grafted chain:

$$S(i) = \left(\frac{4\pi\sigma v}{a^3}\right)^{2/3} \cos^2\left(\frac{\pi i}{2N}\right) \tag{17}$$

where $\sigma = a^2/D^2$ is the grafting density and $v$ the excluded-volume parameter. The average orientational order parameter of the nonuniformly stretched chain is

$$\langle S \rangle = \left(\frac{4\pi\sigma v}{a^3}\right)^{2/3} \tag{18}$$

Thus, the mean order parameter does not depend on the degree of polymerization $N$ (in good solvent) and varies as a 2/3 power of the grafting density. Moreover, $\langle S \rangle$ increases with the solvent quality, which is in agreement with our experimental observations.

The theoretical order profile $S(i)$ stressed in eq 17 is shown in Figure 9a. (We assigned to $S$ to have the same average value as the one measured on sample $P_t$ in hexane.) The theoretical order distribution $P_{th}(S)$ related to $S(i)$ is displayed in Figure 10. In Figure 9b,c (back to Figure 2f), we reported the monodomain and powder

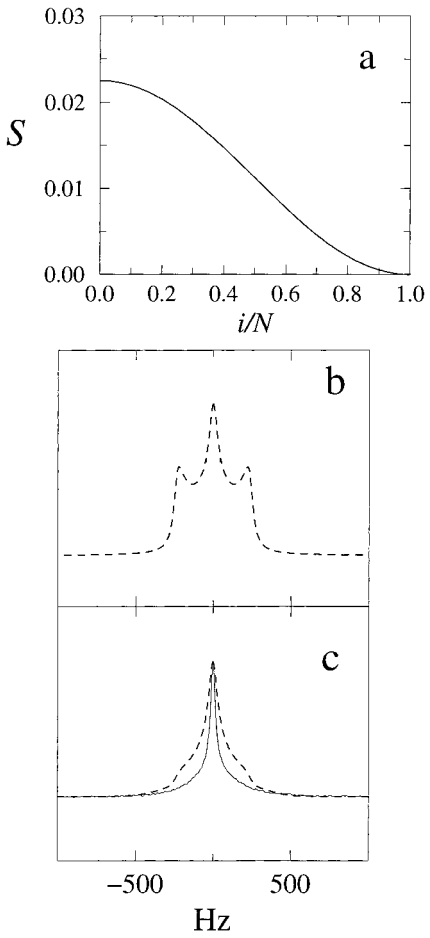


**Figure 9.** (a) Order parameter profile $S(i)$ according to eq 17. $S$ was assigned to have the same mean value as the average $\langle S \rangle$ measured for $P_t$ in hexane. (b) Monodomain spectrum for $\Omega = 90°$ calculated from the order parameter profile $S(i)$ displayed in (a). (c) The 13 MHz $^2$H NMR spectrum of sample $P_t$ in hexane (solid line) and spectrum (dotted line) calculated from the order parameter profile $S(i)$ displayed in (a).

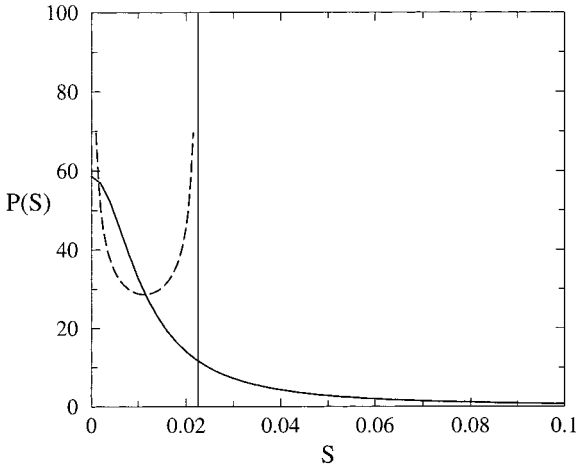


**Figure 10.** Order distribution $P(S)$ for $P_t$ in hexane (solid line). The dashed line is the theoretical order distribution for a grafted layer in good solvent, corresponding to the order profile $S(i)$ (see eq 17) shown in Figure 9a.

spectra simulated from this $P_{th}(S)$. (Note that for the calculation of these spectra the $T_2$ contribution plays a marginal role since the line shape has been found to be fully dominated by the distribution of residual interactions.) Even though the isotropic component is still present, a doublet structure appears on the monodomain spectrum (see Figure 9b). This doublet structure is the source of the peculiar shape of the calculated powder spectrum displayed in Figure 9c. The calculated line shapes are qualitatively different from the experimental spectra observed both for the monodomain $M_t$ in $CCl_4$ (refer to Figure 1b for comparison) and for the porous silica $P_t$ in hexane (Figure 9c). This discrepancy appears even more clearly with the order distributions shown in Figure 10. The experimental order distribution is much broader than the theoretical one.

## V. Concluding Remarks

In this work, grafted PDMS layers immersed in various solvents have been investigated by deuterium NMR. The spectra revealed that the grafted chains have local anisotropic dynamics. A detailed analysis allowed us to determine the distribution $P(S)$ of the characteristic orientational order parameter. The variation of $P(S)$ with the solvent quality gives information about the constraints acting upon the grafted chains.

First of all, it was proved that both in air and in $CCl_4$ (good solvent for PDMS) the normal to the grafting plane is a uniaxial symmetry axis for reorientational motions of the chain segments: the grafted chains are submitted to a uniaxial constraint along **n**. In poor solvent (including air), the average segmental order parameter is negative ($\langle S \rangle < 0$): the chains are squeezed. Furthermore, the line shape analysis shows unambiguously that all the segments throughout the layer feel the confinement: the squeezing constraint is quite uniformly distributed along the chains. On the other hand, in good solvent, the anisotropy increases with the solvent quality, indicating that the order parameter becomes positive ($\langle S \rangle > 0$). This has been interpreted as the result of the strong chain stretching induced by the excluded-volume interaction: the segments tend to be perpendicular to the grafting plane. Unlike in poor solvent, the order parameter is nonuniformly distributed along the chains: unoriented segments coexist with highly oriented ones.

The characterization of the segment dynamics in polymer brushes appears complementary to the determination of the segment concentration profile which can be done by SANS or NR. The transition from poor to good solvent is not reflected by a dramatic change of the concentration profile, as shown by SANS[5] or NR.[6] From the NMR point of view, however, this transition is marked by the change of the order parameter sign and by a qualitative important modification of the distribution $P(S)$ which in particular reveals the presence of isotropic motions in good solvent.

The comparison of our results with the theoretical studies on grafted layers shows that squeezing effects (ignored by the theories) can dominate in poor solvent at low and moderate grafting density. In good solvent, we show strong evidence that the segment dynamics tend to be perpendicular to the grafting plane, in qualitative agreement with the theoretical schemes. However, quantitatively, the order distribution turns out to be much broader than it was predicted. Among the various explanations that could account for these discrepancies, we can mention that the orientational correlations between segments are not taken into account in the models. Moreover, the grafting plane might not be simply described as an impenetrable wall, but short- and long-range interactions should also be considered. For instance, attractive interactions between the chain segments and the substrate may favor a negative order parameter (and so an oblate average conformation of the chains).

It is interesting to note that, from the NMR point of view, the highly swollen brushes and polymer networks are somewhat analogous systems. Spectra obtained with brushes in good solvent resemble those observed on relaxed PDMS networks.[26] The "super Lorentzian" line shape of these (powder) spectra results from both a distribution of end to end vector orientation and a gradient of anisotropy along the cross-linked chains. In swollen networks, the chains are stretched, and the anisotropy of the segment dynamics increases with swelling.[27] The case where a PDMS network is forced to deform along one direction upon swelling appears to be very similar to PDMS brushes, grafted on a planar surface and immersed in a good solvent. In both cases, uniaxial segment dynamics is observed, as revealed by NMR.[28,29]

In view of the interpretation of the anisotropy we have observed for the brushes in good solvent, it would be useful to study the effect of the grafting density and the polymer length. The swelling of labeled (unlabeled) grafted layers by unlabeled (labeled) free polymer chains (of various molecular weight) might also provide us with another way to investigate the orientational correlations. Finally, it would be interesting to extend this study to other polymers—like deuterated polystyrene—in order to change the interaction with the silica and to investigate the effect of the local chain stiffness on the segment ordering.

## References and Notes

(1) Alexander, S. *J. Phys. (Paris)* **1977**, *38*, 983.
(2) de Gennes, P. G. *Macromolecules* **1980**, *13*, 1069.
(3) Milner, S.; Witten, T. A.; Cates, M. E. *Macromolecules* **1988**, *21*, 2610.
(4) Zhulina, E. B.; Borisov, O. V.; Pryamitsym, V. A.; Birshtein, T. M. *Macromolecules* **1991**, *24*, 140.
(5) Auroy, P.; Auvray, L.; Léger, L. *Macromolecules* **1991**, *24*, 2523.
(6) Karim, A.; et al. *Phys. Rev. Lett.* **1994**, *73*, 3407.

(7) Lodge, T. P.; Fredrickson, G. H. *Macromolecules* **1992**, *25*, 5643.
(8) Balsara, N. P.; Perhaia, D.; Safinya, C. R.; Tirell, M.; Lodge, T. P. *Macromolecules* **1992**, *25*, 3896.
(9) Zeghal, M.; Auroy, P.; Deloche, B. *Phys. Rev. Lett.* **1995**, *75*, 2140.
(10) Zeghal, M.; Deloche, B.; Albouy, P-A.; Auroy, P. *Phys. Rev. E* **1997**, *56*, 5603.
(11) Zeghal, M.; Deloche, B.; Auroy, P. *Short and Long Chains at Interfaces*; Editions Frontières: Gif-sur-Yvette, Cedex, France, 1995; p 77.
(12) Cohen-Addad, J. P. *J. Chem. Phys.* **1974**, *60*, 2440. The quadrupolar Hamiltonian is analogous to the dipolar Hamiltonian of a proton pair. The relaxation function for a deuterium nucleus is written in the same way as developed in this reference.
(13) Samulski, E. T. *Polymer* **1985**, *26*, 177.
(14) Abragam, A. *The Principles of Nuclear Magnetism*; Clarendon Press: Oxford, 1961.
(15) Davis, J. H.; Jeffrey, K. R.; Bloom, M.; Valic, M. I.; Higgs, T. P. *Chem. Phys. Lett.* **1976**, *42*, 390.
(16) Cohen Addad, J. P. *Progress in Nuclear Magnetic Resonance Spectroscopy*; Pergamon: New York, 1993; p 25.
(17) Yen, L.; Eichinger, B. E. *J. Polym. Sci.* **1978**, *16*, 121.
(18) Summers, W. R.; Tewari, Y. B.; Schreiber, H. P. *Macromolecules* **1972**, *5*, 12. Hammers, W. E.; Ligny, C. L. *J. Polym. Sci.* **1974**, *12*, 2065.
(19) Halperin, A. *J. Phys. (Paris)* **1988**, *49*, 547.
(20) The layer thickness $h$ in poor solvent can be easily obtained from the average volume fraction $\bar{\Phi}$ (measured by SANS as in ref 5 or estimated by simple weight experiments; see also ref 5). $h = h_0/\bar{\Phi}$ where $h_0$ is the layer thickness measured in air (cf. Table 1). For the solvents used in this study, we have: acetone, $\bar{\Phi} = 0.60$; methanol, $\bar{\Phi} = 0.90$. Thus, for $P_t$ in poor solvent, the layer thickness is smaller than or comparable to $R_g$ ($h/R_g = 0.97$ in acetone and $h/R_g = 0.67$ in methanol).
(21) Chen, Z. Y.; Cui, S. M. *Phys. Rev. E* **1995**, *52*, 3876.
(22) Morse, D. C.; Fredrickson, G. H. *Phys. Rev. Lett.* **1994**, *73*, 3235.
(23) Brinke, G.; Ausserré, D.; Hadziioannou, G. *J. Chem. Phys.* **1988**, *89*, 4374.
(24) Sotta, P.; Deloche, B.; Herz, J. *Polymer* **1987**, *29*, 1171.
(25) Sotta, P. *Trends Macromol. Res.* **1994**, *1*, 291.
(26) Sotta, P.; Deloche, B. *Macromolecules* **1990**, *23*, 1999.
(27) Wenerstrom, H. *Chem. Phys. Lett.* **1973**, *18*, 41.
(28) Deloche, B.; Dubault, A.; Durand, D. *J. Polym. Sci. B* **1992**, *30*, 1419.
(29) Rabin, Y.; Samulski, E. T. *Macromolecules* **1992**, *25*, 2985.

MA981153Y